Journal of Hazardous Materials 480 (2024) 136085

Contents lists available at ScienceDirect

Journal of Hazardous Materials

journal homepage: www.elsevier.com/locate/jhazmat

Research Paper

Co-occurrence of microplastics and microparticles containing Cu and Zn and other heavy metals in sea-surface microlayer in Osaka Bay, Japan

Mi Zhou [a], Issey Osaka [b], Kotaro Hashimoto [b], Chee Kong Yap [c], Christina Emmanouil [d], Takeshi Nakano [a], Hideo Okamura [e,*]

[a] Graduate School of Maritime Sciences, Kobe University, Fukaeminami-machi, Higashinada-ku, Kobe 658-0022, Japan
[b] Department of Pharmaceutical Engineering, Faculty of Engineering, Toyama Prefectural University, Imizu, Toyama 939-0398, Japan
[c] Department of Biology, Faculty of Science, Universiti Putra Malaysia, 43400 UPM Serdang, Selangor, Malaysia
[d] School of Spatial Planning and Development, Aristotle University of Thessaloniki, 54124 Thessaloniki, Greece
[e] Research Center for Inland Seas, Kobe University, Fukaeminami-machi, Higashinada-ku, Kobe, 658-0022, Japan

HIGHLIGHTS

- Metal microparticles pollution in sea-surface microlayer in Osaka Bay was studied.
- Cu, Cu-Zn, Zn, Ti, Sn, Ba and Fe-Mn-Ni microparticles were found.
- 97.8 % of Cu and 52.6 % of Zn microparticles have an acrylic resins matrix.
- High concentrations for Cu (<54,000 mg/kg) and Zn (<13,200 mg/kg) in microparticles were found.
- Highly reliable calibration curves for Cu and Zn in microparticles were applied for micro XRF analysis.

GRAPHICAL ABSTRACT

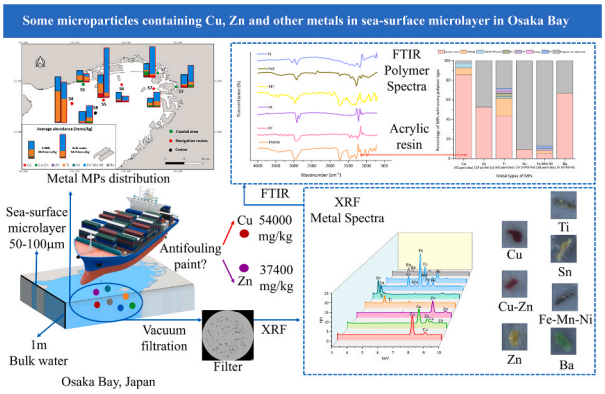

ARTICLE INFO

Keywords:
Metal microparticles
Antifouling paint particles
Microplastics
Sea-surface microlayer
Osaka Bay

ABSTRACT

Antifouling biocides such as Cu, Zn, and organic compounds not only inhibit adhesion of sessile organisms on ship hull but also possess toxicity to non-sessile organisms in marine environment. Thus, we firstly investigated the heavy metals and polymer types of anthropogenic microparticles (MPs) floating in the sea-surface microlayer (S-SML) in Osaka Bay. 7 types of MPs containing different metals (Cu, Cu-Zn, Zn, Ti, Sn, Ba and Fe-Mn-Ni) were found. The polymer type for 97.8 % of Cu and Cu-Zn MPs (41 samples) and 52.6 % of Zn MPs (19 samples) was acrylic resins which are widely used as binders in contemporary antifouling paints for ships; concentrations of 511–54,000 mg/kg for Cu and 95.1–13,200 mg/kg for Zn were found in these MPs. The high metal concentrations found the co-existence of acrylic polymers point towards an origin from antifouling paint particles (APPs). Furthermore, to quantify Cu and Zn concentrations in these MPs based on X-ray fluorescence spectroscopy (μ-XRF), calibration curves obtained from standard paint particles containing different Cu and Zn

* Corresponding author.
E-mail addresses: zhoumi77@163.com (M. Zhou), okamurah@maritime.kobe-u.ac.jp (H. Okamura).

https://doi.org/10.1016/j.jhazmat.2024.136085
Received 22 July 2024; Received in revised form 14 September 2024; Accepted 4 October 2024
Available online 6 October 2024

concentrations and different particle sizes made with similar matrix used in commercial antifouling paint were firstly established, according to which highly reliable Cu and Zn concentrations in MPs were obtained.

1. Introduction

Microplastics (less than 5 mm) pollution in marine environment, firstly highlighted in 1970s, has nowadays become a global concern, due to microplastics small sizes, enormous abundance, ubiquitous distribution, bioavailability and the latent menace they pose to ecosystems [1]. Microplastics are synthetic materials composed by polymers and additives [2], and paint particles also contain consistent components with backbones of polymers such as alkyd, epoxy and acrylic resins [3]. Nevertheless, paint particles are always excluded from the category of microplastics due to the omission of paint in marine litter guidelines [4]. Only recently the International Union for the Conservation of Nature (IUCN) did confirm that marine coatings and antifouling paints are also potential sources of marine microplastics [5]. Noteworthy, compared with microplastics with similar sizes, paint particles exhibit higher chemical toxicity due to their greater mobility of toxic metal ions and higher concentration of hazardous inorganic additives in the matrix [6].

The occurrence of floating paint particles in surface seawater has also been reported over the past decade. Paint fragments with a size range of 0.3–23 mm presented a total abundance approximately 30 times higher than that of plastics in the sea surface waters around the Antarctic Peninsula; red paint fragments deriving from hulls were the most abundant [7]. In addition, among the total microplastics in the surface seawater, micro-sized paint particles accounted for 28.42 % in the Goiana Estuary of Brazil [8], 7.7 % in the Mediterranean Sea [9], 12 % around oceanic islands of the Western Tropical Atlantic Ocean [10], 55.45 % in the Sinop Sarikum Coast of the Southern Black Sea [11], 25.8 % in the Chabahar Bay, Gulf of Oman [12], 33 % in the South China Sea [13] and 15.21 % in the Jiangsu coastal area in China [14], respectively. These micro-sized paint particles are mostly suspected to originate from the boat maintenance and cleaning. Moreover, marine traffic and shipping activities seem to produce higher amounts of antifouling and marine paint-related microparticles. Abundant micro-sized Polymethyl Methacrylate (PMMA) resins have been detected in navigation routes in Osaka Bay, Japan, with an abundance of 903 ± 921 items/kg in the sea-surface microlayer (S-SML), accounting for 95.1 % of total microplastics [15], and at the shipping lane in the northwestern region of the German Bight, with a concentration of 1032 ppt in surface seawater, accounting for 83 % of total microplastics [16], respectively. Massive amounts of micro-sized alkyd resins have also been found in the southern coast of Korea, with an abundance of 171 items/L in S-SML, accounting for 81 % of total measured microplastics [17]. Given that abundant microplastics in navigation routes in Osaka Bay have been found, this study continues to investigate the microparticles (MPs) that may be related to antifouling and marine paints in Osaka Bay.

Until now, usually the assessment of marine microplastics related to ships as mentioned above was based on the analysis of polymer types, while the investigation on heavy metals therein was neglected. It is known that polymers such as acrylic, alkyd and epoxy resins are always used as the plastic backbone of marine paints, however, they can also be used in a variety of other plastic products. Therefore, it is important to know whether microplastics originate from marine paints or not; this cannot be assumed just by simply identifying their polymer component and additional metal analysis should follow. For improving the identification on paint-related MPs, both the polymer types and the metal component with each microparticle were measured to explore the co-occurrence of microplastics and metal MPs in this study.

Many heavy metals are related to antifouling and marine paints. For marine paints, Ti, Ba, Cr, Fe, Sn and Pb are commonly used in pigments, and Cr is used in anticorrosive agents [3]. For antifouling paints, Cu and Zn, are used as biocides to prevent fouling and attachment of marine organisms on hulls [18]- as such it is safe to assume that they reflect the occurrence of antifouling paint particles (APPs). Cu, Zn, Ag, Cd, Cr, Ni, Pb, Sn, Mn and Ni have all been detected in antifouling paint residues collected from the hard-standings of a marine leisure boat facility in Plymouth, UK [19]. In Singapore's coastal environment, Zn was the most abundant metal and it most likely originated from the antifouling paint from boats [20]. Given the greater surface area exposed to aqueous medium when in particulate form, metals are predicted to leach from APPs more rapidly [21], which can undoubtedly cause sustained ecotoxicity to aquatic organisms. In this study, MPs containing metals (metal MPs) in Osaka Bay were investigated in detail; especially Cu-Zn-based MPs were analyzed to explore their association with antifouling paints.

Particulate Cu, Fe and Ni in S-SML was found in 1972 in Narragansett Bay in USA [22]. Besides, suspended particulate matter was significantly enriched in Cd, Cr, Cu, Ni, Pb and Zn in S-SML in Singapore's coastal environment [20]. The S-SML with a thickness of 50–100 μm is the uppermost layer of the ocean [20]. As S-SML is the interface between seawater and atmosphere, heavy metals therein can also enter the atmosphere and enrich the atmosphere aerosol [22]. In their turn, atmospheric aerosols can be transported many km away depending on the wind and meteorological conditions. As such, anthropogenic particulate metals pollution at remote Antarctic regions due to transportation of aerosols by circumpolar wind had been verified [23]. Thus, metal MPs transported from S-SML to atmosphere can cause widespread transmission and pollution. The opposite mechanism can also be noted; S-SML can also accumulate particulate metals from atmospheric deposition [20], then these particulate metals can sink and spread into water column and sediment due to gravitational settling. Since abundant microplastics are prone to accumulate in S-SML due to the surface tension, much more than in water column [15,17], metal MPs in S-SML may present wide range and large abundance. In view of this, S-SML was preferentially investigated in this study.

Up to present, there has been no research on the polymer composition of metal MPs in S-SML to identify the relationship between metal MPs and microplastics or APPs. For exploring the existence of metal MPs in S-SML in Japan, an important inland sea, the Osaka Bay, where abundant microplastics have previously been found, served as the study area. The purpose of this study was to (1) investigate the metal types, abundance, distribution and paint-related potential sources of these metal MPs in different depths in surface seawater (S-SML and bulk water) and in different marine spatial zones (coastal area, navigation routes and center of the bay), (2) identify the polymer types of these metal MPs, then measure their concentrations for Cu and Zn that are related to metal biocides in antifouling paint to explore their association with APPs. Significantly, to quantify Cu and Zn concentrations in MPs based on X-ray fluorescence spectroscopy (μ-XRF), calibration curve obtained from commercial antifouling paints containing different concentrations for Cu and Zn and similar polymeric matrix with that of anthropogenic MPs was established, and highly reliable and accurate Cu and Zn concentrations in MPs can be measured by this way compared to traditional methods which had neglected the polymeric matrix of MPs. This study is the first to investigate the co-occurrence patterns of metal MPs and microplastics in the sea-surface microlayer (S-SML), and suggest that the pollution of MPs with high concentration for Cu and Zn in S-SML is worth to attention.

2. Materials and methods

2.1. Sampling sites

The site examined in the present study is Osaka Bay in Japan. Osaka Bay located in the western Japan is elliptical in shape, with its major and minor axes being about 60 and 30 km, respectively. For Osaka Bay, the Akashi Strait on the west can convey seawater from the Harima Nada, the estuary of the Yodogawa on the east is connected by the Shin-Yodogawa River that flows from southwest of the Lake Biwa (Japan's largest lake), and the Kii Chanel on the south can lead to the exchange of seawater with the Pacific Ocean. In general, Osaka Bay is connected to numerous other water recipients in Japan and may be a representative candidate for the overall water pollution status throughout the western Japan. Moreover, there are many shipyards around the Hanshin Industrial Zone in the northeast of the bay, which can generate antifouling paint fragments during hull maintenance and cleaning. In addition, the cruise, ferry and merchant ships can also produce antifouling and marine paint MPs along the shipping routes in the bay. Finally, the industrial and residential areas along the coast have also become potential sources of metal MPs. Hence, 8 sampling sites within the Bay were selected according to different water zones. As shown in Fig. 8, S1, S2 and S3 are located in the coastal area, S4, S5, S6 and S7 are located in the navigation routes and S8 is located in the center of the bay.

2.2. Reagents

All chemicals and reagents were of analytical grade. 30 % Hydrogen Peroxide (H_2O_2, Wako Pure Chemical Industries, Ltd., Osaka, Japan) was used to digest organic matters on filter samples. For measuring Cu and Zn content, hydrochloric acid (12 M, 35 % HCl, Wako Pure Chemical, Osaka, Japan) and nitric acid (13.4 M, 61 % HNO_3, Kanto Chemical, Ltd., Osaka, Japan) were diluted with ultrapure water (UPW) to prepare 1 M HCl, 1 M HNO_3 and 0.015 M (= 0.1 %) HNO_3, and aqua regia was prepared by mixing 3 parts of HCl (12 M, 35 %) with 1 part of HNO_3 (13.4 M, 61 %). The standard Cu solution (Cu1000, 1000 mg/L, Wako Pure Chemical Industries, Ltd., Japan) was diluted to 40, 20, and 10 μg/L (ppb) by 0.1 % HNO_3, and the standard Zn solution (Zn 1000, 1000 mg/L, Wako Pure Chemical Industries, Ltd., Japan) was diluted to 3, 1.5, and 0.75 mg/L (ppm) by 0.1 % HNO_3 for preparing a calibration curve to be used with flameless atomic absorption spectrometry (FLAAS).

2.3. Metal MPs sampling and processing

The collecting method and laboratory pre-treatment of MPs on filters were carried out according to Zhou et al. [15]. Briefly, the metal MPs were collected during the years 2021–2023 in surface seawater in Osaka Bay. The sampling information is shown in Table S1. An electric rotating drum sampler and pump sampler were used to collect S-SML and bulk water (1 m under the sea surface), respectively. Both S-SML and bulk water were sequentially filtered by stainless-steel sieves (φ10 cm) (JIS Z 8801, Tokyo Screen, Japan) with mesh-sizes of 500, 125 and 53 μm, then the waters were returned to the10 L tank. MPs captured on these sieves were rinsed into bottles by UPW. After to laboratory, MPs in these bottles and tanks were filtered by PTFE filters (POPMF-1000, 10 μm, Wintec, Kobe, Japan) with diameters of 47 mm and 142 mm, respectively. MPs on filters had been classified by size ranges of 10–53, 53–125, 125–500 and > 500 μm. These filters with MPs of every size range were kept in petri dishes and dried at 60 ℃ for 12 h, then 30% H_2O_2 solution was added onto these filters to digest organic matters for 1 week. After this, MPs on these filters were rinsed by UPW and filtered through nylon filters with corresponding mesh sizes respectively, and MPs captured on these nylon filters were rinsed into PTFE filter (H100A013A, ADVANREC, 1 μm, φ13 mm, Wintec, Kobe, Japan) for the last filtering. Finally, all filters were dried at 60 ℃ for 12 h in an oven (D-450 FA, AS ONE, Osaka, Japan) and used for microscopic observations.

2.4. Detection and identification of metal MPs

MPs on filters were observed and their metal types were identified by the X-Ray Fluorescence Spectrometry (μ-XRF: XGT-900, HORIBA, Kyoto, Japan). Compared to inductively coupled plasma-mass spectroscopy (ICP-MS) that has been widely used to measure metal elements in seawater in previous relevant studies [20,24], μ-XRF can detect multiple types of metals in one solid particle simultaneously. For MPs of > 500, 125–500 and 53–125 μm, all MPs on filters were determined by the μ-XRF and their metal types and corresponding abundances were recorded. For MPs of 10–53 μm, due to their high abundances and laborious counting, just five squares of the filter were randomly selected, and metal MPs therein were identified and counted as mentioned above. One square was 1.4 × 1.4 mm^2 and five squares were approximately 1/8 of the total filtered area (78.5 mm^2). Some metal MPs were selected to be observed by Infrared Microscope (AIM-9000, SHIMAZU, Kyoto, Japan, the same position on the filter was used) and their polymer types were detected by the Fourier Transform Infrared Spectrometer (μ-FTIR: IRTracer-100, SHIMADZU, Kyoto, Japan). The relevant process of water sampling and laboratory treatment is shown in Fig. S1.

2.5. Preparation of standard Cu-Zn-based APPs

To create calibration curve between metal concentration and corresponding Fluorescence X-ray intensity, the standard Cu-Zn-based APPs were prepared by mixing commercial Cu-Zn-based acrylic antifouling paint (named "Paint 1″, R Copper Red, Nippon Paint, Ltd., Tokyo, Japan) with Ti-based PMMA marine coating (named "Paint 2″, Dainippon Paint, Ltd., Osaka, Japan) by a volume ratio of 10:90. All the paints used in this stduy are shown in Table S2. This mixed paint was then diluted by the Ti-based PMMA marine coating (Paint 2) exponentially for 7 times; finally 8 kinds of mixed paints with concentration gradients for Cu and Zn were obtained in total. The paints were identified as SS1, SS2, SS3, SS4, SS5, SS6, SS7 and SS8 with a Cu-Zn-based paint volume percentage of 10%, 5%, 2.5%, 1.25%, 0.625%, 0.312%, 0.156% and 0.0781%, respectively. These 8 kinds of mixed paints were evenly applied on baking paper, then peeled off into fragments after air-drying. These paint fragments were put into specialized crushing containers and immersed in liquid nitrogen for 5 min, then crushed into APPs through a freezing crusher (Freeze crusher μT-48, TAITEC, Saitama, Japan) using the vertical vibration of the crushing apparatus at 1200 rpm for 5 min. The pulverized APPs were sieved through a stainless-steel sieve cascade (φ10cm) (JIS Z 8801, Tokyo Screen, Japan) with mesh sizes of 500, 125 and 53 μm in turns. Thus, APPs of SS1–SS8 of size ranges of < 53, 53–125, 125–500 and > 500 μm were obtained.

2.6. Determination of fluorescence X-ray intensity for Cu and Zn of standard APPs

The standard APPs of SS1–SS8 described in 2.5 with size ranges of < 53, 53–125, 125–500 and > 500 μm, 32 samples (4 sizes × 8 concentrations) in total, were stored in different dishes, respectively. Every APPs sample was taken out by micro spoon then distributed on a double-sided tape (1.5 ×1.5 cm) pasted onto a plastic cover. The Fluorescence X-ray intensity for Cu and Zn of each sample was determined by the "Poly Capillary" method of μ-XRF. Considering that the diameter of capillary for beam of Fluorescence X-ray was 100 μm, for samples of > 500 and 125–500 μm, the particles surface can be completely covered within the irradiation range of Fluorescence X-rays from capillary. While for the samples of < 100 μm, part of the Fluorescence X-ray beam fails to penetrate the particles and falls into non-sample space. Thus, more particles of < 100 μm should be measured for obtaining sufficient Fluorescence X-ray intensity data with larger range of variation.

Therefore, APPs of 5000, 500–5000, 500, 130–500, 130, 120, 110, 100, 90, 80, 70, 60, 50 μm were selected and the corresponding Fluorescence X-ray intensity was measured and recorded.

2.7. Determination of Cu and Zn concentration (mg/kg) of standard APPs by FLAAS

All plastic- and glassware were soaked in 1 M HCl for at least 24 h before used then rinsed with UPW. About 50 mg of every made standard APPs sample (>500 μm) of SS1–SS8 was weighed by an electronic balance (HTR-80, Yushima Ltd., Japan) and then digested in 10 mL of aqua regia at 85 ℃ for 2 h in covered 100 mL Pyrex beakers [25]. After cooling, the contents (residual APPs and aqua regia) were transferred into volumetric flasks and diluted to 25 mL by 0.015 M (0.1%) HNO_3, then filtered by PTFE filter (H100A047A, ADVANREC, 1 μm, φ47 mm). Considering the high concentrations for Cu and Zn, all digestates should be diluted to ensure that their absorbance (ABS) values for Cu and Zn fall lower than that of 40 ppb Cu solution and 3 ppm Zn solution in the calibration curve (described in 2.2). As such, 0.5 mL of the digestates of SS1–SS8 were diluted 4000, 2000, 2000, 500, 500, 200, 200, and 100 times respectively for the measurement of Cu ABS, and 50, 30, 30, 10, 5, 5, 0 and 0 times respectively for the measurement of Zn ABS. The diluted digestates of SS1–SS8 were identified as S1–S8 correspondingly.

The ABS values for Cu and Zn in the standard Cu and Zn solutions with different concentrations diluted by 0.1 HNO_3 were measured by flameless atomic absorption spectrophotometry (FLAAS) (Z-2710, Hitachi Ltd., Japan) to prepare the calibration curve (described in 2.2). The ABS values for Cu and Zn in S1–S8 solutions were also measured by FLAAS, then the concentrations for Cu and Zn in S1–S8 solutions were calculated according to the calibration curve and their ABS values.

When measuring the ABS, about 20 μL of solution sample was injected into pyrotube HR with a graphite furnace, ABS was monitored at 324.8 nm of Cu with lamp current 7.5 mA and 307.6 nm of Zn with lamp current 5 mA. During the measuring process, the drying at 80–140 ℃ lasted for 40 s, the ashing at 600 ℃ for Cu and 300 ℃ for Zn lasted for 20 s, and the atomizing at 2400 °C for Cu and 2200 °C for Zn lasted for 5 s [26]. The measurement for every sample was repeated 3 times and the average values of ABS were recorded. Concentrations (mg/kg) for Cu and Zn in standard APPs of SS1–SS8 were calculated according to the concentrations for Cu and Zn in S1–S8, their dilution factor, the volume of digestates (25 mL) and the total quantities (about 50 mg) of APPs of SS1–SS8.

2.8. Determination of Cu and Zn concentrations (mg/kg) in metal MPs

For standard APPs of SS1–SS8, their calibration curves between metal (Cu and Zn) concentrations (mg/kg) and corresponding Fluorescence X-ray intensity (cps/mA) of APPs with different sizes (5000, 500–5000, 500, 130–500, 130, 120, 110, 100, 90, 80, 70, 60, 50 μm) were created. Since the Fluorescence X-ray intensity values for Cu and Zn in metal MPs in Osaka Bay had been measured by μ-XRF, the corresponding concentrations for Cu and Zn in these metal MPs then could be calculated by these calibration curves. The relevant process of measurement of concentrations for Cu and Zn in standard APPs of SS1–SS8 and metal MPs in Osaka Bay is shown in Fig. S2.

2.9. Data analysis

QGIS 3.38.0 (QGIS.ORG, https://qgis.org/ja/site/) was used for mapping sampling sites and Osaka Bay that are shown in Fig. 8. All the data analyses were performed in SPSS 19.0 (IBM, New York, NY, USA) and Origin 2021 (OriginLab, Northampton, MA, USA). The curves of polymer spectra were visualized by EZ OMNIC. All the figures were drawn in Excel and Origin 2021. Regarding statistical comparisons, for MPs with all kinds of metals, differences in their abundance at different sampling sites and zones both in S-SML and in bulk water were assessed by the Mann-Whitney U test and one-way ANOVA followed by Tamhane's T2 post-hoc test, while differences in abundance among different kinds of metal MPs were also assessed by Mann-Whitney U test. In addition, the correlations between several parameters of the metal MPs were examined by Pearson's correlation through Origin. Principal component analysis (PCA) was performed through Origin in order to describe the experimental system with a new set of reduced variables deriving from the initial parameters.

3. Results and discussion

3.1. Types and sources of metal microparticles

Through the μ-XRF detection, 7 main kinds of metal components were detected in MPs both in S-SML and bulk water in Osaka Bay, i.e., Cu, Cu and Zn (Cu-Zn), Zn, Ti, Sn, Fe and Mn or Ni (Fe-Mn-Ni) and Ba. The spectra and figures of each representative metal MP are shown in Fig. S3 and S4. Consistently low Zn Fluorescence X-ray intensity indicated low Zn content in these Cu-Zn MPs, as such only Cu Fluorescence X-ray intensity values in these MPs were measured in the subsequent experimental steps. These metal MPs may originate from dumping of industrial and household waste from urban drainage [27] and atmospheric fallout [20], but they may also stem from the antifouling and marine paints used on boats and ships [3]. In addition, as microplastics can also adsorb trace metal ions from their surrounding seawater [28], metals detected in some microplastics may originate from this procedure rather than the metals being already presented in marine paints or APPs. Even so, the accumulation of trace metals onto these microplastics due to adsorption may still cause negative impacts on marine life [29]. Moreover, compared to similarly sized microplastics, paint particles always present higher chemical toxicity due to the presence of hazardous metals [6].

3.2. Polymer types of metal MPs

Considering that abundant PMMA MPs were detected in our previous study [15], some samples already examined via μ-FTIR were further selected and detected by pyrolysis-Gas chromatography/ Mass Spectrometry (py-GC/MS) for a more accurate qualitative analysis on the residual PMMA MPs. The qualitative detection of PMMA confirmed that some PMMA MPs were indeed lost due to the blowing of airflow under full vacuum during the first observation by μ-XRF, but some PMMA MPs still remained on the filters. The relevant experimental methods and results are shown in Supplementary Information 1 and Fig. S5.

As described in 2.4, the polymer types of metal MPs were detected by μ-FTIR after being observed and positioned by μ-XRF. Filters were observed to detect and count metal MPs for the first time by μ-XRF under full vacuum. Some metal MPs were flown away and lost inevitably due to the violent airflow during vacuum pumping. After the first observation and counting, the metal MPs remaining on filters were observed for the second time by μ-XRF under parteral vacuum, and their positions on the filter were marked for the purpose of detecting their polymer composition on the same position on the filter by μ-FTIR. Since frequent and quick sample exchange can be conducted under parteral vacuum without stopping the vacuum pumping, the partial vacuum state was selected for time-saving during the second μ-XRF observation rather than the full vacuum state. Considering the massive abundance and time-consuming detection for MPs of 10–53 μm, the polymer type detection was performed on metal MPs with size ranges of > 53 μm only.

Since Cu and Zn are closely related to biocides in APPs, all the residual Cu, Cu-Zn and Zn MPs on filters were examined by μ-FITR to identify their polymer types to explore their polymeric association with APPs. For metal MPs with size ranges of > 53 μm, during the first observation under full vacuum, 190 items of Cu, Cu-Zn MPs and 106 items of Zn MPs were detected, while just 41 items of Cu, Cu-Zn MPs and 19 items of Zn MPs were detected on the filters during the second

observation. This means that approximately 80 % of Cu, Cu-Zn and Zn MPs were blown away and lost due to the airflow blowing under full vacuum. In addition, a certain number of Ti, Sn, Fe-Mn-Ni and Ba MPs were selected from massive residual metal MPs to measure their polymer composition to determine their association with microplastics and paint particles. The results (percentage of metal MPs containing each kind of polymer) are shown in Fig. 1. For the metal MPs that had also their polymer type identified, information on their pictures and spectra measured by μ-XRF and μ-FTIR, and the corresponding Fluorescence X-ray intensity data for Cu-Zn-based MPs is shown in Supplementary Information 2.

Among 41 items of Cu and Cu-Zn MPs, 35 items belonged to the acrylic resins and 3 items belonged to the PMMA resins. Since PMMA is also categorized as an acrylic resin, it can be deduced that the acrylic resin-based MPs accounted for 93 % of total Cu-based MPs. At present, the acrylic resin-based self-polishing coatings are the most used ones in antifouling on ships; cuprous oxide (Cu_2O) is characterized as one of the main antifouling agents [30]. Therefore, some of the 38 items may well represent APPs that originated from the self-polishing antifouling paints on ships. 2 items of Cu-based MPs exhibited the polymer type PA6 and the polymer type PE-PP with a mixture of 4:1, which may originate from the antifouling paint on the experiment ship [15].

Among 19 items of Zn MPs, 10 items belonged to the acrylic resins and accounted for 52.6 % of all Zn MPs. Since the ban of tributyltin in antifouling paints, Zinc pyrithione (ZnPT) has become one of the most frequently used alternative biocides [31]. In addition, zinc acrylate resin is also one of the most useful resins used as polymeric matrix for antifouling paint [32]. In the current manufacturing process of acrylic antifouling paints in Japan, once the carbon group connecting two ester bonds is replaced by Zn, the hydrolyzed polymer of acrylic-zinc is formed and antifouling paints with excellent film renewal and antifouling properties can be obtained [33]. Besides, zinc oxide (ZnO) is used as a pigment or a booster of biocides in antifouling paints. To sum up, once related to APPs, the Zn MPs with acrylic polymeric matrix may reflect the biocides component of ZnPT, the copolymer composition of acrylic-zinc, and the ZnO used as booster or pigment in acrylic antifouling paints.

As shown in Fig. S6, S7 and S8, the μ-XRF and μ-FTIR spectra of some Cu and Zn MPs with acrylic resins in Osaka Bay were contrasted with these of selected standard commercial Cu-Zn-based antifouling paints in Japanese paint market; the consistency of the compared spectra indicated the same metal and polymer component of these anthropogenic MPs to those in antifouling paints.

Among 60 items of Ti MPs, 26 items belonging to the acrylic resins (43.4 %) and 11 items belonging to the PMMA resins (18.3 %) were found. For these items terrestrial plastics and metal adsorption may be their potential sources, especially they may also originate from the protecting coatings on topside and superstructures of ships if an association with marine paints is assumed [15]. In addition, PA6:PE-PP, PU, PE, Epoxy and PS types accounted for 1.7 %, 3.3 %, 1.7 %, 1.7 % and 1.7 % in abundance among total Ti MPs, respectively. These polymers have also been widely used in the manufacturing of all kinds of plastic products, paints and coatings. Here only the paint-related potential sources of these Ti MPs are discussed. More than 70 % of clear coating layers from original vehicle manufacturers contain PS [34]. PU coatings is the most significant class of industrial paints related to outdoor painted sculptures [35]. Compared to other synthetic resins, epoxy resins dominate in the sector of anti-corrosion coatings due to their longterm corrosion avoidance and chemical resistance [36]. Moreover, low-density polyethylene (LDPE) has also been used as binder for marine anticorrosive coatings [37]. Nanoparticles of TiO_2 are not used only as pigments but they also act as additives that improve mechanical strengths and the ability of anti-microbial, anti-corrosive and self-cleaning of properties [38]. Therefore, if we assume a paint particle origin, Ti MPs with polymeric matrix here may reflect a diverse sources of paints including the antifouling and anticorrosive paints used on surfaces of ships and marine structures in water environment, and the coatings on vehicle surface and buildings on land.

Among 32 items of Sn MPs, just 3 items belonging to the acrylic type MPs (9.38 %) were identified and the polymer types of the rest of samples did not match with polymers data recorded in the library base of μ-FITR. Sn MPs without polymers seemed to occupy most of the

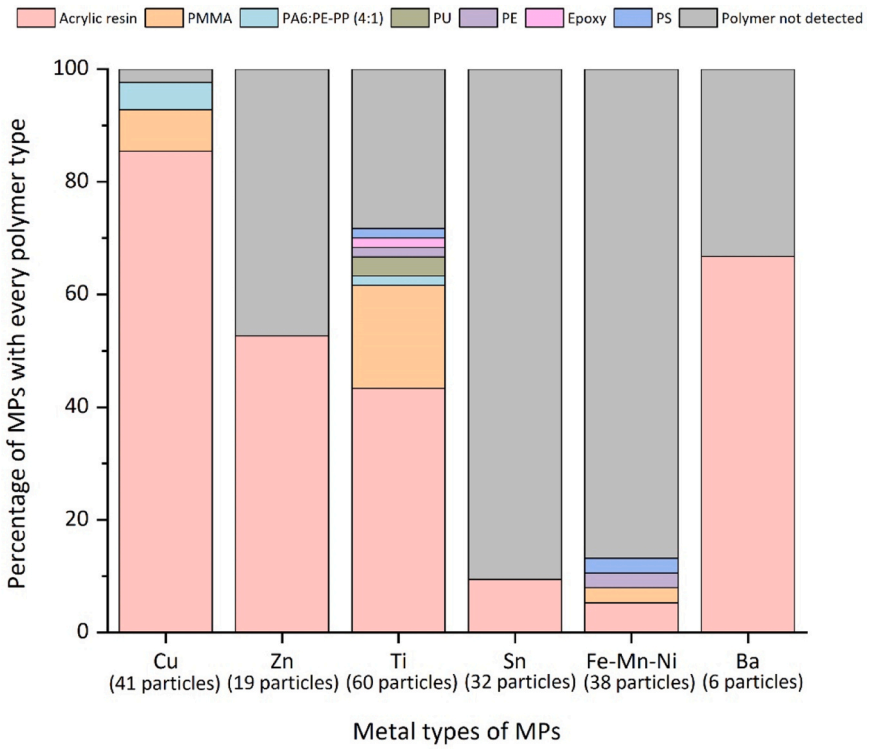

Fig. 1. Percentage of MPs with every polymer type accounted in every kind of metal MPs.

proportion in marine environment.

Among 38 items of Fe-Mn-Ni MPs, 2 items of acrylic MPs (5.26 %), 1 item of PMMA MP (2.63 %), 1 item of PE MP (2.63 %) and 1 item of PS MP (2.63 %) were detected. The rest of Fe-Mn-Ni MPs (86.85 %) that did not show matching polymers may be inorganic metal MPs. Owing to the lower density of polymers compared to metals, Fe-Mn-Ni MPs without polymer components may present a relative higher density, which can lead their gathering in bulk water rather than in S-SML, further affecting their vertical distribution in the water column.

Among 6 items of Ba MPs, 4 items belonging to the acrylic resins (66.7 %) were detected. Considering the least abundance of Ba MPs among all metal MPs, just 6 Ba MPs were discovered for the measurement of polymer types, while the high proportion of Ba MPs with acrylic resins may suggest that most Ba MPs floating in marine environment have polymeric matrix.

3.3. Cu and Zn concentrations (mg/kg) in metal MPs

Cu and Zn MPs with acrylic resins may reflect the presence of APPs, however, they may also derive from adsorption of metal ions onto aged microplastics from the surrounding water environment [28]. Therefore, concentrations for Cu and Zn in these MPs should be measured, and only acrylic MPs containing high concentrations for Cu or Zn may actually be characterized as APPs.

As described in 2.5, 2.6, 2.7 and 2.8, the calibration curve for standard APPs (SS1–SS8) between metal concentration (mg/kg) and Fluorescence X-ray intensity (cps/mA) is prepared for measuring the concentrations for Cu and Zn in the 41 items of Cu-based MPs and the 19 items of Zn MPs. For exploring whether the extraction of Cu and Zn by aqua regia can be affected by APPs sizes, SS1 APPs with size ranges of $>$ 500, 125–500, 53–125 and $<$ 53 μm were selected to measure their concentrations for Cu and Zn. The values of ABS for Cu and Zn in the digestates, the calculating process and concentrations for Cu and Zn in SS1 APPs with 4 size ranges are as shown in Table S3–7. Especially shown in Table S7, the concentrations for Cu and Zn extracted from SS1 APPs with different sizes presented no discrepancy between them ($p > 0.05$). This verified that the APPs sizes cannot affect the extraction of Cu and Zn therein, therefore, only APPs of $>$ 500 μm for SS1–SS8 samples were selected to determine their concentrations for Cu and Zn. The corresponding values of ABS for Cu and Zn in digestates and the concentrations for Cu and Zn in SS1–SS8 APPs (>500 μm) are shown in Table S8–19. The average values of concentrations for Cu and Zn in SS1–SS8 (>500 μm) (Table S20) were used as the data in Y-axis of the calibration curve. Meanwhile, the Fluorescent X-ray intensity values for Cu and Zn in SS1–SS8 APPs with the size of 5 mm, 500–5000, 500, 130–500, 130, 120, 110, 100, 90, 80, 70, 60 and 50 μm measured by μ-XRF (Table S21and 22) were used as the data in X-axis of the calibration curve. Based on the values of concentrations for Cu and Zn and Fluorescent X-ray intensity for standard APPs of SS1-SS8 with different sizes, the calibration curve between their metal concentrations (mg/kg) and Fluorescent X-ray intensity values (cps/mA) were drawn as shown in Figs. 2 and 3.

For Cu, Cu-Zn MPs (41 items) and Zn MPs (19 items) larger than 50 μm, their Fluorescent X-ray intensity values were recorded in Supplementary Information 2. According to these Fluorescent X-ray intensity values and the calibration curves, their concentrations for Cu and Zn were calculated as shown in Table 1 and Table 2. For one Cu or Zn MP, its Fluorescent X-ray intensity value was brought into two calibration curves whose size parameters were adjacently larger and smaller than that of the MP, then two corresponding metal concentration values were calculated and the average value was taken as the final concentration for Cu or Zn. The Cu concentration in 41 items Cu-based MPs ranged from 511–54,000 mg/kg in one MP, i.e. the mass percentage of Cu in MPs ranged from 0.05–5.4 % w/w. Meanwhile, among 17 items of floating micro paint flakes ($>$ 60 μm) found in the North Atlantic Ocean, their Cu concentration ranged from $<$ 52.9 to 6960 mg/kg in one flake (0.005–0.7 % w/w) [39], which was lower than that in this study. Similarly, the Zn concentration in 19 items of Zn MPs in this study ranged from 95.1–13,200 mg/kg (<0.01–1.3 % w/w) in one MP, which was higher than that the result of Zn concentration ranged from $<$ 38.2 to 37,400 mg/kg in one paint flake (<0.004–3.8 % w/w) in the North Atlantic Ocean [39].

Until now there is no universal method to identify Cu and Zn MPs as APPs. For the 17 items of paint flakes in the North Atlantic Ocean, some alkyd or epoxy-based flakes with Cu concentrations $>$ 824 mg/kg were identified as Cu-based APPs [39], according to which, 37 items acrylic

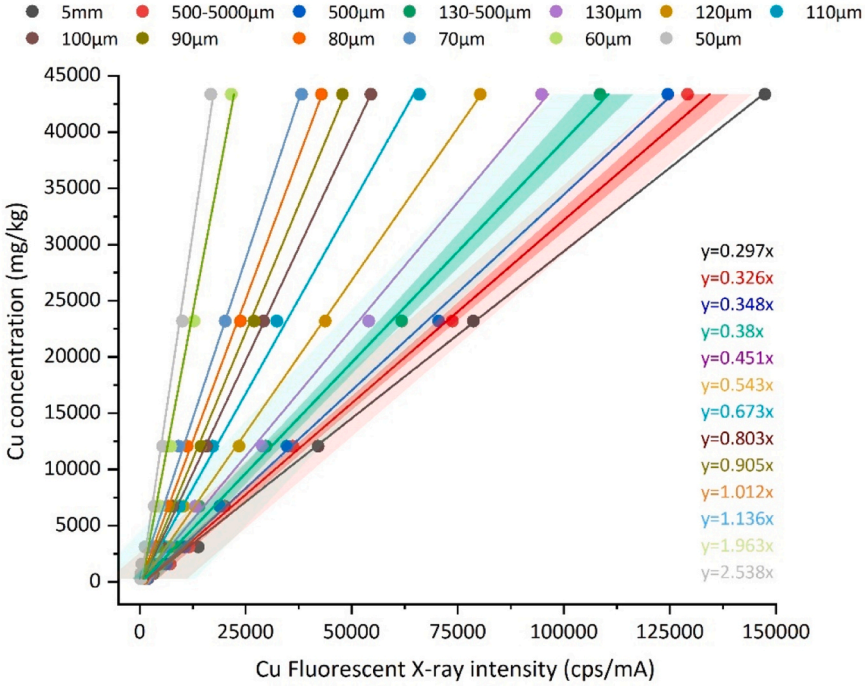

Fig. 2. Calibration curve between concentration and Fluorescence X-ray intensity for Cu in standard APPs (SS1–SS8) with different sizes.

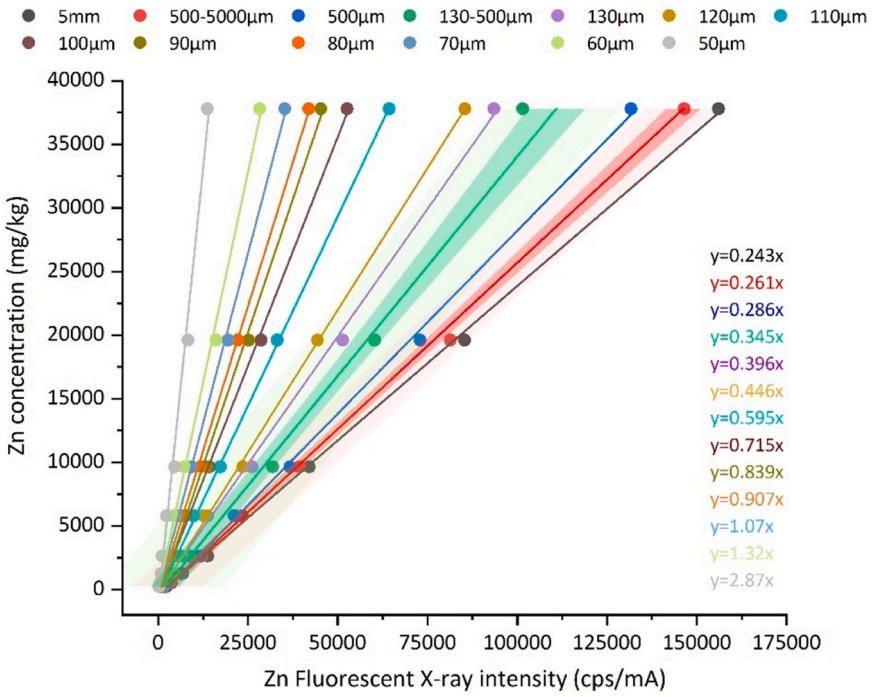

Fig. 3. Calibration curve between concentration and Fluorescence X-ray intensity for Zn in standard APPs (SS1–SS8) with different sizes.

Table 1
Cu concentrations (mg/kg) in 41 items of Cu MPs.

Depth	Size (μm)	Coastal area			Navigation routes				Center
		1	2	3	4	5	6	7	8
S-SML	> 500			2700		54,000 32,000 960			2900
	125–500	5610				23,000 5800 3100 1900			4900 1400
	53–125					34,000			
Bulk water	> 500		2100 1300			5900			
	125–500			6600 4400 1700		35,000 30,000 28,000 18,000 4300 4200 3200 2900 1700 1400 1200 900 810 526 511		10,000	12,000
	53–125			3000	10,700			15,000 4200 1200	

MPs with Cu concentration > 810 mg/kg in this study maybe also identified as Cu-based APPs. Although no relevant references were available for Zn MPs, some of the Zn MPs in this study maybe characterized as Zn-based APPs according to their high Zn concentrations and acrylic resins that are always used as binders and polymeric matrix in antifouling paints.Significantly, high concentrations for Cu and Zn in metal MPs in this study seems to reflect the Cu-Zn-based biocides or pigments that already exist in APPs rather than originate from metal absorption on aged microplastics from water.

Altogether, high concentrations of Cu and Zn in MPs in S-SML and bulk water in Osaka Bay were detected. Given the continuous leaching of Cu and Zn from MPs and their ecotoxicity to marine organisms, these MPs with high concentrations for Cu and Zn should be concerning. Furthermore, highly reliable and accurate concentrations for Cu and Zn

Table 2
Zn concentrations (mg/kg) in 19 items of Zn MPs.

Depth	Size (μm)	Coastal area			Navigation routes				Center
		1	2	3	4	5	6	7	8
S-SML	>500				635				
	125–500			1090	1970				1090
									591
									718
									217
									95.1
	53–125	4500			5600				
Bulk water	>500	5100	2210						
	125–500							12,300	127
	53–125			7080		13,200	3950	1200	
				10,200					

were obtained through the calibration curve shown in Figs. 2 and 3, due to the commercial antifouling paints with similar whose polymeric matrix (acrylic resin) was the same as that of anthropogenic MPs. This can provide insights for measurement of Cu and Zn concentrations in MPs in future research.

3.4. Percentage distribution of all metal MPs and their potential sources

The percentage distribution of all metal MPs among different sampling zones and depths was conducted according to their abundances. As shown in Fig. 4, navigation routes contributed most of metal MPs loads with the percentage of 65.1 %. Furthermore, 26.2 % and just 8.7 % of metal MPs originated from coastal area and from bay center respectively. Among all types of metal MPs, Fe-Mn-Ni MPs were the most abundant, accounting for 60.4 %, while minor ones were Ti MPs (28.2 %), Cu MPs (4.5 %), Cu-Zn MPs (3.9 %), Sn MPs (1.4 %), Zn MPs (1.3 %) and Ba MPs (0.3 %). For Cu, Cu-Zn, Zn, Ti, Sn MPs, their abundances in both S-SML and bulk water were at a similar level, while the Fe-Mn-Ni MPs abundance in bulk water was about twice higher than that in S-SML. This is probably the main reason for the higher abundance level of all metal MPs in bulk water. Ba MPs were found in bulk water only.

It was also shown that 55.6 % Cu MPs, 20.5 % Cu-Zn MPs and 92.3 % Zn MPs originated from navigation routes, so if some of these Cu-Zn-based MPs originate from APPs from antifouling paints due to shipping activities, their generation mechanism is discussed as follows. Most contemporary antifouling paints contain Cu(I)-based biocides (commonly cuprous oxide). Moreover, although zinc oxide is also used as the principal biocidal pigment sometimes, it is more generally used in combination with Cu(I) as a booster to increase the toxicity of the latter by 200-fold [21]. For contemporary self-polishing antifouling paints, during navigation, the soluble biocides are released to prevent the attachment of organisms to the coat surface. At the same time a new fresh area of coating is uncovered for subsequent release of biocides along with the continuous hydrolysis of the acrylic matrix depending on the shear of seawater flow [40]. The mechanical disturbance of coatings is one mechanism that can generate APPs [6], during which, theoretically the polymeric matrix of antifouling paint has been hydrolyzed, and the copolymer film becomes brittle accompanying the dissolution of biocides [41]. Considering that APPs are generated more passively with the general wear and tear (erosion) of hull [6], the brittle polymer matrix containing Cu and Zn-based biocides may fall off from the coating surface by the abrasion of seawater shear force, then further break into APPs. In addition, another mechanism of the formation of APPs is the UV degradation of the binding polymer that leads to the weathering of coatings [6,42]. The weathering and abrasion of ship

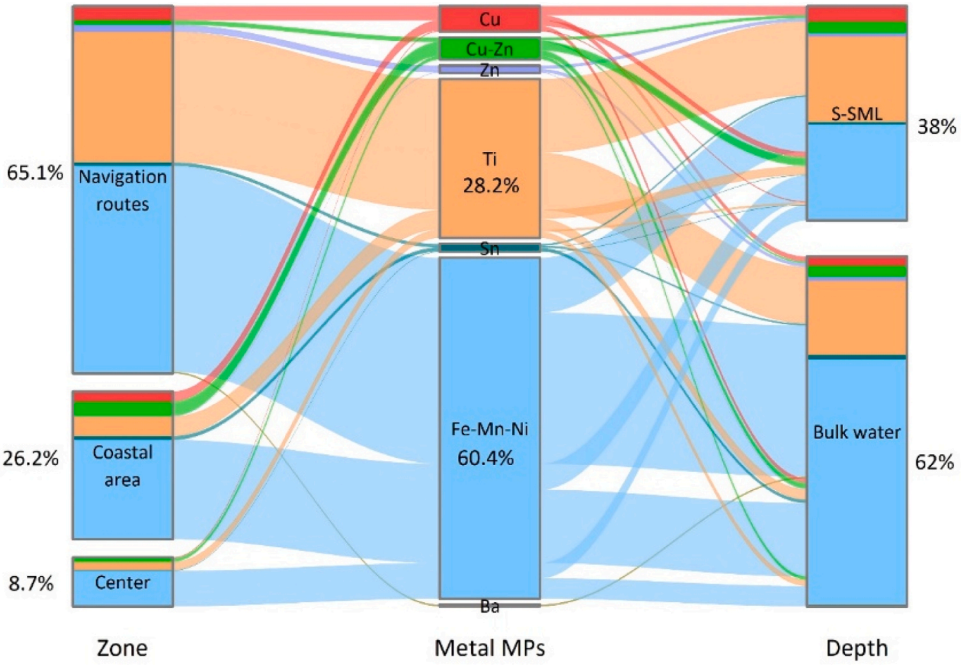

Fig. 4. Alluvial diagram of the distribution of each kind of metal MPs in abundance at different sampling zones both in S-SML and bulk water.

paints above the waterline can also generate APPs [39]. High salinity in seawater may increase the rate of the aging process for polymers compared with freshwater [43], therefore, antifouling paints above the waterline are prone to be weathered more easily when contacted with seawater then further break into APPs. In addition, the present results also show that about 40 % Cu MPs, 64.1 % Cu-Zn MPs and 7.69 % Zn MPs originated from coastal area of the bay. In this case, if we assume that these MPs were APPs, their sources may be linked to repainting and cleaning of hulls in shipyards, especially for leisure boats where paint emissions are not well regulated. During the processes of scraping, sanding, stripping, sand-blasting and hydro-blasting of spent coatings for hull maintenances, significant quantities of toxic APPs are transported to aquatic environment [6]. These APPs floating in water cannot be hydrolyzed in relatively static seawater which does not impose shear stress; as such the residue may persist in the water environment for quite long [15]. It is noted however that compared to navigation routes, coastal area contributed much fewer Cu and Zn MPs.

Most of Ti MPs (82.3 % of total) also originated from the navigation routes. If associated with shipping activities, some of these MPs may derive from marine paints applied to the topside on ships. White color is used extensively on the superstructures of ships [44] and titanium dioxide (TiO_2) is applied in paint as a white pigment due to its high refractive index [38]. It is notable that the annual consumption of TiO_2 in the production of paint is 75 % greater than that of all other pigments put together [45]. Grey paints on the topside of hulls are also pigmented with TiO_2 [46], especially for admiralty ships in British navy [45]. Moreover, Rutile TiO_2 and Anatase TiO_2 are the main component of the titanium white pigment which is widely used in marine coatings in the contemporary Japanese paint market [47,48]. Marine sites are characterized by high humidity and salinity [49], which can make Ti-based marine paints fall off into seawater due to weathering more easily. Compared to antifouling paint that contain Cu and Zn as biocides, TiO_2 is less ecotoxic and more environmental-friendly since it is well embedded in the coating matrix and cannot leach easily [50]. Therefore, Ti MPs in water environment may produce fewer repercussions to aquatic biota. In addition, Ti with high concentration of 1046.01–175513.36 mg/g (dry weight) in sediments was detected in Lake Garda [51]. As shown in Fig. S9, S10 and S11, the consistency of the compared spectra by μ-XRF and μ-FTIR indicated that Ti MPs had the same metal and polymer component as Ti-based marine and antifouling paints prevailing in Japanese paint market, thus, some Ti MPs are likely to stem from marine paints.

Sn MPs from navigation routes and coastal area accounted for 42.9 % and 50 %, respectively. Although Sn is also used as hardening catalyst in contemporary antifouling paints in Japan [52], given that most Sn MPs in this study do not have a polymeric matrix (Fig. 1), the Sn detected in MPs seemed to not associate with APPs but rather with metal adsorption from the surrounding seawater. Organotin compounds, especially Tributyltin (TBT) had been used as antifouling biocides most widely before 1989 and they have been gradually regulated and finally banned for use on shipbuilding due to their adverse effects on marine organisms and repercussions on water environment [53]. However, in recent years, TBT with concentrations 4.4–28 ng/L in water samples at Tanabe Bay in Japan was detected and these levels are deemed toxic for gastropods in seawater [54]. Besides, Sn was also found in micro paint flakes in North Atlantic Ocean with the concentration ranged from 387 mg/kg to $<$ 1900 mg/kg in one flake [39], and in plastics in sediments of Lake Garda (38.84–972.25 μg /g) in one plastic sample [51]. Thus, Sn MPs in this study may reflect the residual and adsorption of residual organotin formulations from historic applications of antifouling paints, and their hazardous and negative impacts on marine ecosystems may continuously exist.

Fe-Mn-Ni MPs contribution from navigation routes, coastal area and center was 60.4 %, 29.1 % and 10.5 %, respectively. The abundance of Fe-Mn-Ni MPs in bulk water was about twice as high than that in S-SML. As shown in Fig. 4, most Fe-Mn-Ni MPs without polymeric matrix are likely to deposit due to their higher density compared to microplastic then gathering in bulk water. Coupling of Fe and Mn in MPs prevailed in this study as shown in Supplementary Information 2, and a similar Fe-Mn association was also observed in groundwater of Changchun city, China [55]. Both Fe and Mn are abundant elements in the earth crust, and the source of Fe-Mn nodules are mainly aquifer clay layers [55]. In addition, the Fe-Mn MPs seem to be related with waste effluents from industries such as steel plants due to anthropogenic activities [24]. Thus, most of the Fe-Mn MPs in this study may have little connection with paint flakes and ship activities. However, polymer components such acrylic resins, PMMA, PS, PE and PVC were still detected in some Fe-Mn MPs (Supplementary Information 2 and Fig. 1). This shows a certain correlation between the Fe-Mn coupling and microplastics, which needs to be investigated further.

It is noteworthy that Ni is also coupled with Fe-Mn in some MPs in this study, and this seems to have not been reported in relevant research so far. Here, 2 items of Fe-Mn-based acrylic MPs also contained Ni simultaneously (Supplementary Information 2). Although this may have been caused by metal absorption, the possibility that these Fe-Mn-Ni MPs with acrylic matrix are associated with marine and paints cannot be excluded. Mn and Ni visibly attached to paint fragments that were collected from a marine boat maintenance facility in Plymouth, England reflected the components of metallic base materials of the hulls [19]. In view of this, the co-occurrence of Ni with Fe-Mn in MPs with acrylic or other polymeric matrix may reflect the metallic substrates of hulls attached to antifouling or anticorrosive paints. It is known that carbon and alloy steels are widely used in shipping due to their good mechanical properties and low cost [56], and the surface modification technology is applied on these steel substrates to improve their mechanical performance, corrosion and wear resistance without affecting its comprehensive properties [57]. Laser beams are widely used in surface modification of many kinds of metals [58] utilizing the method of surface alloying and surface cladding [59]. The laser cladding technology has attracted great attention in recent decades and has been widely used to improve the surface properties of alloys [60]. At present, Fe-based and Ni-based alloy powders are mainly used in laser cladding technology to obtain the Fe and Ni-based composite alloy coatings combined with the alloy matrix [61], and Mn has also been added in laser cladding to improve the non-magnetic properties of the composite coatings [62]. In addition, Mn is also the main element in carbon steel with a mass percentage of 0.2–1.5 %. Once the protective coatings on hulls are worn and damaged due to impaction and aging, the base steel can come in contact with corrosive seawater, which then results in a continued corrosion attack to metallic materials [63]. The corroded metallic base materials containing Fe, Ni or Mn are removed and peeled off by the flowing seawater then they may break into MPs. It had been verified that Fe found in micro paint flakes in the North Atlantic Ocean may come from the corroded fragments of an underlying steel substrate of the hull [39]. Thus, a small portion of Fe-Mn-Ni MPs with polymeric matrix in this study may originate from the exfoliation of steel substrates of hulls that had been corroded by seawater, or from the metal absorption. This may explain why the most abundant loads of Fe-Mn-Ni MPs were found in navigation routes.

Finally, regarding Ba MPs, the lowest percentage originated from navigation routes and these MPs were found only in the bulk water. Barium sulphate ($BaSO_4$) has been used as pigments [64] in historical TBT antifouling paint and extenders in antifouling [65] and anticorrosive paints [66]. Meanwhile, Ba has also been found in micro paint flakes in North Atlantic Ocean with a concentration of $<$ 1860 mg/kg to $<$ 30, 000 mg/kg in one flake [39], in antifouling paint fragments from a large marine boat maintenance facility in Plymouth, with a concentration of 1050 $\pm$ 89 mg/g in one fragment [19], and in plastics in sediments of Lake Garda with a concentration of 38.84–972.25 mg/g in one plastic sample [51]. As such, the Ba MPs at navigation routes in this study may also reflect the occurrence of MPs of antifouling and anticorrosive paints.

3.5. Principle component analysis (PCA) of metal MPs

Although it is difficult to confirm the complex potential sources of these metals that originated from different anthropogenic and nature pathways, some associations among different metals may provide insights about the attributions of metal MPs through multivariate analysis. Principal component analysis (PCA) was performed as described in 2.9, and the parameters examined were the abundance of each type of metal MPs at different sampling sites and zones both in S-SML and in bulk water among all samplings (22 collections for S-SML and 25 collections for bulk water). The PCA results of the loadings are shown in Fig. 5. The three-factor solution explained 64.7 % of the variance, where PC1 contributed 29.4 % of the total variance with positive loadings of Cu and Zn, PC2 contributed 19.8 % of the total variance with positive loadings of Ti and Sn, and PC3 contributed 15.5 % of the total variance with positive loadings of Fe-Mn-Ni, Zn and Ba. A hypothesis on sources and spatial patterns of distribution of all the metal MPs in the study area can be proposed according to this analysis.

This study focuses on exploring the sources of metal MPs related to marine and antifouling paints, and therefore the results of PCA was explained based on the metal composition of the paints in the following discussion. The strong positive loadings of Cu and Cu-Zn on PC 1 undoubtedly reflected the occurrence of Cu-based APPs, which originated from the maintenance and cleaning in dry dock and shipyard and the navigating activities in shipping lane. PC2 was characterized by strong positive loadings of Ti and Sn; this may be linked to the common source of Ti and Sn in pigments and additives in marine paints. The positive loadings of Fe-Mn-Ni, Zn and Ba in PC3 indicated the source of metal MPs stemmed from the metallic base materials attached to paint component including corrosion inhibitors of zinc phosphate and extenders of barium sulphate. Overall, PCA analysis verified the hypothesis of the marine and antifouling paint-related source origins of the detected metal MPs.

3.6. Co-occurrence pattern of metal MPs and microplastics

The abundance, size ranges, polymer types, distribution of microplastics in both S-SML and bulk water in Osaka Bay have been investigated in our previous study [15]. In the present research, the co-occurrence of metal MPs and microplastics in the same sampling sites was analyzed through Pearson's correlation analysis. As shown in Fig. 6, there was no significant correlation between the abundance of any kind of metal MPs and the distance from land of each sampling site. In addition, the abundance of every kind of metal MPs in S-SML and bulk water presented no significant discrepancy ($p > 0.05$). While metal MPs can still be captured and float in S-SML due to the surface tension therein even though metals always have a higher density than seawater. For Cu, Zn Ti, Sn and Fe-Mn-Ni MPs, there is a significant negative correlation between abundance and size decreased ($R^2 = -0.186$ for Cu, -0.189 for Zn, -0.152 for Ti, -0.144 for Sn, -0.204 for Fe-Mn-Ni, respectively, $p < 0.05$). Metal MPs of smaller sizes are more, in relation to total MPs numbers and their loads are prone to increase as they decompose into smaller MPs. Furthermore, for Cu, Zn, Ti and Sn MPs, their abundance was positive correlated to the abundance of polymer containing microplastics ($R^2 = 0.358$ for Cu, 0.244 for Zn, 0.438 for Ti, 0.183 for Sn, respectively, $p < 0.05$), which revealed their associations with microplastics. The Pearson correlation showed the co-occurrence pattern between metal MPs and microplastics. This may indicate that some of the existing Cu, Zn, Ti and Sn MPs may represent the debris from antifouling and marine paints and coatings. On the other hand, it may also demonstrate metal adsorption on microplastics, which corroborates the function of microplastics as pollutant carriers. This might be especially true for Sn-related to Tributyltin in historical antifouling paint formulations-which once adsorbed on microplastics, may continue to impact marine organisms.

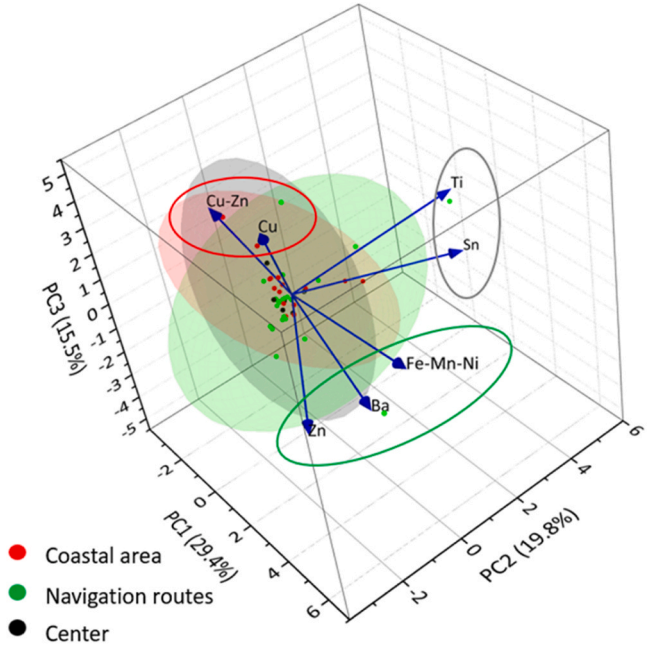

Fig. 5. Principle component analysis (PCA) of all kinds of metal MPs in surface water.

The correlation between each kind of metal MPs abundance and abundance of microplastics with each polymer type was also assessed as shown in Fig. 7. It is noted that in our previous study, considering the overwhelming abundance PMMA MPs, acrylic resins were also classified as PMMA MPs. In the present study however, Cu MPs with acrylic resins did not present positive correlation with PMMA MPs abundance; this may be because we did not specially record acrylic resins abundance in the previous study. Most notably, there was a strong positive correlation between PMMA MPs and Ti MPs in abundance ($R^2 = 0.3$, $p < 0.05$). This illustrates that these Ti MPs also exhibit a PMMA polymeric matrix, this can be also verified in Fig. 1, where PMMA polymeric MPs accounted for about 60 % in total Ti MPs. The high degree of co-occurrence of Ti and PMMA in MPs may reveal the pollution caused by Ti-based acrylic paints due to complex pathways and sources, including paints from terrestrial paints from exterior of buildings or from marine and antifouling paints in ocean. In addition, PS MPs also presented a positive correlation with Ti and Sn MPs. PS MPs are widely used in coatings in vehicle manufacturing, but they are also contained in terrestrial road marking paints, which is considered as a significant source of paint fragment and debris in several Japanese cities [67]. Therefore, the high correlation between Ti and Sn MPs and PS MPs may reflect the application of Ti pigment and Sn hardening catalysts in road marking paints. Regarding adsorption of metals on microplastics, given that the PMMA, PS and PET are common types of microplastics in marine environments, whether they are more likely to serve as carriers for metal adsorption needs to be determined in future research.

3.7. Spatial abundance distribution of total metal MPs

As shown in Fig. 8, metal MPs were detected by μ-XRF at all sampling sites. The average abundance (MPs items in 1 kg seawater) of metal MPs was 38.8 items/kg in S-SML and 54.3 items/kg in bulk water, respectively, while there was no significant difference between them ($p > 0.05$, Mann-Whitney U test). Also, metal MPs abundance was distributed without significant difference between coastal area, navigation routes and center ($p > 0.05$, one-way ANOVA Tamhane's T2 post-hoc test), which indicated that metal MPs have a relatively uniform distribution in abundance in surface seawater in Osaka Bay. Notably, the abundance of microplastics in S-SML was significantly higher than that in bulk water in our previous study [15], which may spread the

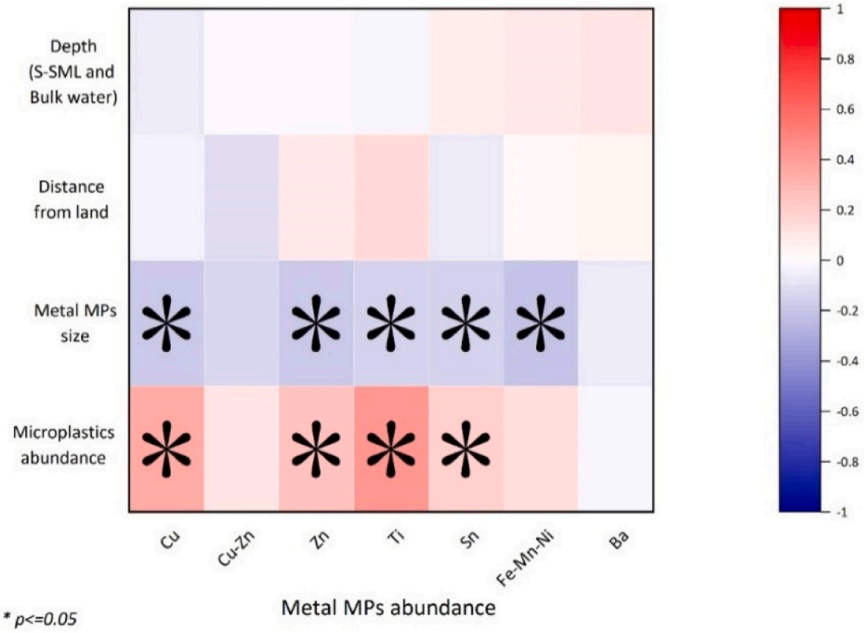

Fig. 6. Pearson's correlation analysis between metal MPs abundance and microplastics abundance, metal MPs sizes, distance from land and depth (S-SML and bulk water).

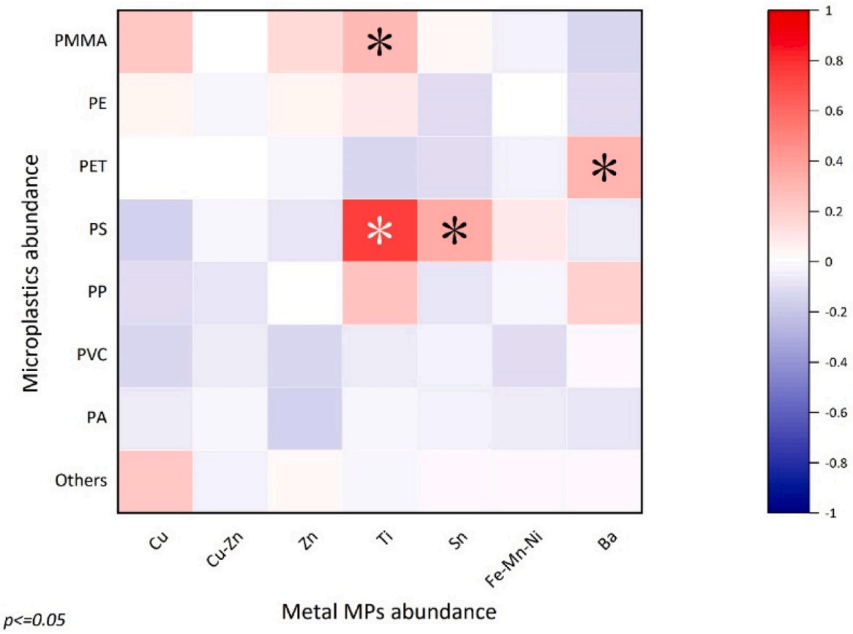

Fig. 7. Pearson's correlation analysis between metal MPs abundance and abundance of microplastics with every kind of polymer type.

microplastic pollution into the atmosphere and water column. Thus, the occurrence of metal MPs in S-SML was investigated specially in this study, while they presented no significance in abundance with those in bulk water. Higher density of metals may lead these metal MPs tend to deposit and gather in bulk water rather than float in S-SML. Even so, metal MPs in S-SML may still cause the metals transfer into atmosphere and water column, metal MPs in S-SML especially for Cu-Zn-based MPs should be noticed.

As clearly shown in Fig. 8, Ti-MPs and Fe-Mn-Ni MPs contributed huge amounts of metal MPs at all sampling sites. Both in S-SML and bulk water, Fe-Mn-Ni MPs abundance was significantly higher than that of Ti MPs ($p < 0.05$, Mann-Whitney U test) and of other metal MPs ($p < 0.01$, Mann-Whitney U test), meanwhile, Ti MPs abundance was also significantly higher than that of Cu, Cu-Zn, Zn, Sn and Ba MPs ($p < 0.01$, Mann-Whitney U test). Fe was the most abundant metal found in metal MPs in this study. This was mostly consistent with previous relevant research in the Bohai Bay in China, where mass concentration of Fe was higher than that of other metals in suspended particulate matter [68].

4. Conclusion

Our research investigated the co-occurrence of microplastics and metal MPs in the S-SML in Osaka Bay for the first time. The study provided information on metal types, abundance, distribution and polymer types of metal MPs in marine environment. Cu, Cu-Zn, Zn, Ti, Sn, Fe-Mn-Ni and Ba MPs were detected. Notably, most Cu-Zn-based MPs exhibited

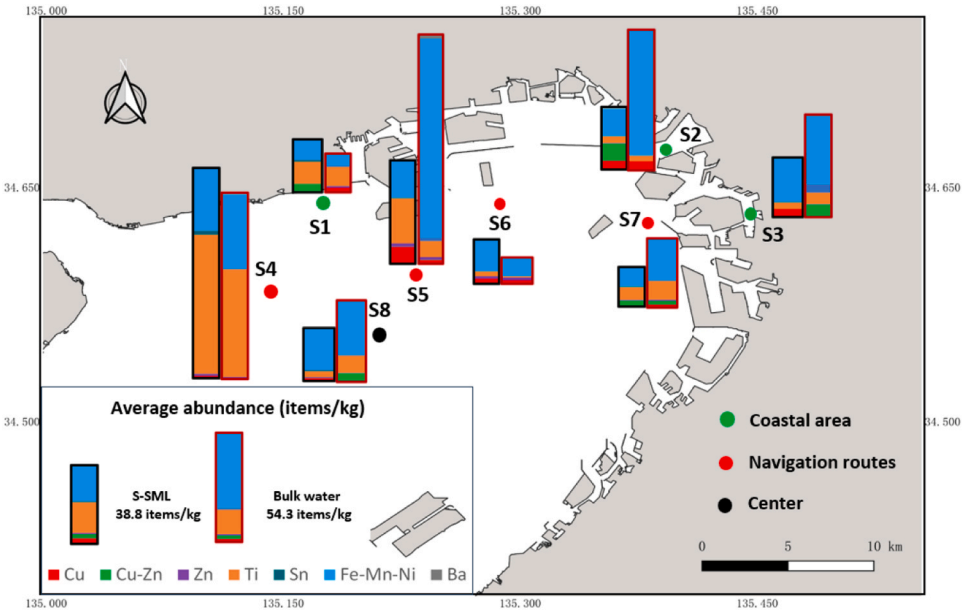

Fig. 8. Sampling sites and spatial distribution of average abundance of metal MPs.

a polymeric matrix of acrylic resins that are widely used as binders in antifouling paints. Given the application of Cu and Zn as biocides in antifouling paints, some acrylic MPs containing high concentrations of Cu and Zn may originate from antifouling paints and their pollution potential should be investigated. The abundances of Fe-Mn-Ni MPs and Ti MPs were significantly higher than these of other types of metal MPs. Metal MPs were always positively correlated with microplastics abundance. Moreover, Ti MPs exhibited diversity in their polymeric matrix and presented positive correlation with PMMA microplastics abundance, which may be related to the Ti-based marine paints. Coupling between Ni and Fe-Mn in some acrylic MPs may reflect the substrates of hulls attached to antifouling or anticorrosive paint flakes. These results provide new insights in understanding the paint-related sources of metal MPs with acrylic matrix. Significantly, highly reliable and accurate concentrations for Cu and Zn in MPs were measured by calibration curves obtained from standard paint particles with similar matrix based on μ-XRF.

Environmental implication

Compared to microplastics of similar size, antifouling paint particles (APPs) always show stronger ecotoxicity to aquatic organisms due to facilitation to mobility of antifouling biocides such as Cu, Zn, and organic compounds. This study firstly investigates the co-occurrence of metal microparticles (MPs) and microplastics in the sea-surface microlayer (S-SML). Some acrylic resin MPs containing high concentrations of Cu (< 5.4 %) and Zn (< 1.3 %) are likely related to APPs. The Cu and Zn concentrations in the MPs were calculated from a calibration curve using commercial antifouling paint particles as the standard matrix, and are highly reliable value.

CRediT authorship contribution statement

Hideo Okamura: Writing – review & editing, Methodology, Investigation, Funding acquisition, Conceptualization. **Takeshi Nakano:** Supervision. **Christina Emmanouil:** Writing – review & editing, Supervision. **Chee Kong Yap:** Supervision. **Kotaro Hashimoto:** Methodology. **Issey Osaka:** Writing – review & editing, Methodology. **Mi Zhou:** Writing – original draft, Visualization, Validation, Software, Methodology, Investigation, Data curation.

Declaration of Competing Interest

The authors declare that they have no known competing financial interests or personal relationships that could have appeared to influence the work reported in this paper.

Data availability

Data will be made available on request.

Acknowledgements

We would like to thank Professor Koji HAMASAKI, AORI, The University of Tokyo, for helping us making the RDS-KU1 to collect samples from the S-SML. We also thank Katsumi AOYAMA and Keisuke KITAJIMA, Kobe University Training Ship HAKUO. This work was supported by the New Energy and Industrial Technology Development Organization, Moonshot Research and Development Program (JPNP 18016-20333325) to H.O.

Appendix A. Supporting information

Supplementary data associated with this article can be found in the online version at doi:10.1016/j.jhazmat.2024.136085.

References

[1] Cole, M., Lindeque, P., Halsband, C., Galloway, T.S., 2011. Microplastics as contaminants in the marine environment: a review. Mar Pollut Bull 62, 2588–2597.
[2] Arthur C, Baker J, Bamford H,. Proceedings of the international research workshop on the occurrence, effects and fate of microplastic marine debris. Sept 9–11, 2008, NOAA Technical Memorandum NOS-OR&R30; 2009.
[3] Gaylarde, C.C., Neto, J.A.B., Fonseca, E.Md, 2021. Paint fragments as polluting microplastics: a brief review. Mar Pollut Bull 162, 111847.
[4] OSPAR Commission, 2010. Guideline for monitoring marine litter on the beaches in the OSPAR maritime area. OSPAR Commission, London.
[5] IMO, 2019. Hull scrapings and marine coatings as a source of microplastics. International Maritime Organization,, London, UK.
[6] Turner, A., 2021. Paint particles in the marine environment: an overlooked component of microplastics. Water Res X 12, 100110.
[7] Lacerda, A., Rodrigues, L., Sebille, E., Rodrigues, F., Ribeiro, L., Secchi, E.R., et al., 2019. Plastics in sea surface waters around the Antarctic Peninsula. Sci Rep 9, 3977.
[8] Lima, A.R.A., Costa, M.F., Barletta, M., 2014. Distribution patterns of microplastics within the plankton of a tropical estuary. Environ Res 132, 146–155.

[9] Suaria, G., Avio, C.G., Mineo, A., Lattin, G.L., Magaldi, M.G., Belmonte, G., et al., 2016. The Mediterranean Plastic Soup: synthetic polymers in Mediterranean surface waters. Sci Rep 9, 37551.
[10] Ivar do Sul, J.A., Costa, M.F., Fillmann, G., 2014. Microplastics in the pelagic environment around oceanic islands of the Western Tropical Atlantic Ocean. Water Air Soil Pollut 225, 2004.
[11] Öztekin, A., Bat, L., 2017. Microlitter pollution in sea water: a preliminary study from Sinop Sarikum coast of the southern Black Sea. Turk J Fish Aquat Sci 17, 1431–1440.
[12] Aliabad, M.K., Nassiri, M., Kor, K., 2019. Microplastics in the surface seawaters of Chabahar Bay, Gulf of Oman (Makran coasts). Mar Pollut Bull 143, 125–133.
[13] Wang, T., Zou, X.Q., Li, B.J., Yao, Y.L., Zang, Z., Li, Y.L., et al., 2019. Preliminary study of the source apportionment and diversity of microplastics: taking floating microplastics in the South China Sea as an example. Environ Pollut 245, 965–974.
[14] Wang, T., Li, B.J., Yu, W.W., Zou, X.Q., 2021. Microplastic pollution and quantitative source apportionment in the Jiangsu coastal area, China. Mar Pollut Bull 166, 112237.
[15] Zhou, M., Yanai, H., Chee, Y.K., Emmanouil, C., Okamura, H., 2023. Anthropogenic microparticles in sea-surface microlayer in Osaka Bay, Japan. J Xenobiot 13, 685–703.
[16] Dibke, C., Fischer, M., Scholz-Böttcher, B.M., 2021. Microplastic mass concentrations and distribution in german bight waters by pyrolysis−gas chromatography−mass spectrometry/thermochemolysis reveal potential impact of marine coatings: do ships leave skid marks? Environ Sci Technol 55, 2285–2295.
[17] Song, Y.K., Hong, S.H., Jang, M., Kang, J.H., Kwon, O.Y., Han, G.M., et al., 2014. Large accumulation of micro-sized synthetic polymer particles in the sea surface microlayer. Environ Sci Technol 48, 9014–9021.
[18] Muller-Karanassos, C., Turner, A., Arundel, W., Vance, T., Lindeque, P.K., Cole, M., 2019. Antifouling paint particles in intertidal estuarine sediments from southwest England and their ingestion by the harbour ragworm, Hediste diversicolor. Environ Pollut 249, 163–170.
[19] Singh, N., Turner, A., 2009. Trace metals in antifouling paint particles and their heterogeneous contamination of coastal sediments. Mar Pollut Bull 58, 559–564.
[20] Cuong, D.T., Karuppiah, S., Obbard, J.P., 2008. Distribution of heavy metals in the dissolved and suspended phase of the sea-surface microlayer, seawater column and in sediments of Singapore's coastal environment. Environ Monit Assess 138, 255–272.
[21] Turner, A., 2010. Marine pollution from antifouling paint particles. Mar Pollut Bull 60, 559–564.
[22] Piotrowicz, S.R., Ray, B.J., Hoffman, G.L., Duce, R.A., 1972. Trace metal enrichment in the sea-surface microlayer. J Geophys Res 77, 5243–5254.
[23] Marina-Montes, C., Pérez-Arribas, L.V., Escudero, M., Anzano, J., Cáceres, J.O., 2020. Heavy metal transport and evolution of atmospheric aerosols in the Antarctic region. Sci Total Environ 721, 137702.
[24] Kar, D., Sur, P., Mandal, T., Saha, T., Kole, R.K., 2008. Assessment of heavy metal pollution in surface water. Int J Environ Sci Tech 5 (1), 119–124.
[25] Holmes, L., Turner, A., 2019. Leaching of hydrophobic Cu and Zn from discarded marine antifouling paint residues: Evidence for transchelation of metal pyrithiones. Environ Pollut 157, 3440–3444.
[26] Okamura, H., Kano, K., Yap, C.K., Emmanouil, C., 2022. Floating particles with high copper concentration in the sea-surface microlayer. Environ Sci Pollut R 29, 29535–29542.
[27] Sadiq, M., 1992. Toxic metal chemistry in marine environments. Marcel Dekker, New York.
[28] Vedolin, M.C., Teophilo, C.Y.S., Turra, A., Figueira, R.C.L., 2018. Spatial variability in the concentrations of metal in beached microplastics. Mar Pollut Bull 129, 487–493.
[29] Jasna, M.L., Jelena, L., Pero, T., Dubravka, B.V., Jasna, Š., 2018. Levels of trace metals on microplastic particles in beach sediments of the island of Vis, Adriatic Sea, Croatia. Mar Pollut Bull 137, 231–236.
[30] Zhang, H., Kong, F., Chen, Y., Zhao, X., Tang, Y., Zuo, Y., 2023. Degradation of two anti-corrosion and anti-fouling coating systems in simulated diurnal cycling immersion. Coatings 13, 389.
[31] Soon, Z.Y., Jung, J.H., Jang, M., Kang, J.H., Jang, M.C., Lee, J.S., et al., 2019. Zinc pyrithione (ZnPT) as an antifouling biocide in the marine environment—a literature review of its toxicity, environmental fates, and analytical methods. Water Air Soil Poll 230, 310.
[32] Ni, C.H., Feng, K., Li, X., Zhao, H.Z., Yu, L.M., 2020. Study on the preparation and properties of new environmentally friendly antifouling acrylic metal salt resins containing indole derivative group. Prog Org Coat 148, 105824.
[33] Tanino S, Hayashi Y. Antifouling Coating Composition, Antifouling Coating Film, Base Material Provided with Antifouling Coating Film, Method for Product Same, and Antifouling Method WO2018/003136, 1 April 2018; 2021. (In Japanese).
[34] Yang, S.H., Shen, J.Y., Chang, M.S., Wu, G.J., 2012. Quantification of vehicle paint components containing polystyrene using pyrolysis-gas chromatography/mass spectrometry. Anal Methods 4, 1989–1995.
[35] Defeyt, C., Langenbacher, J., Rivenc, R., 2017. Polyurethane coatings used in twentieth century outdoor painted sculptures. Part I: comparative study of various systems by means of ATR-FTIR spectroscopy. Herit Sci 5, 11.
[36] Aggarwal, L.K., Thapliyal, P.C., Karade, S.R., 2007. Anticorrosive properties of the epoxy–cardanol resin-based paints. Prog Org Coat 59, 76–80.
[37] Singh, S.K., Tambe, S.P., Raja, V.S., Kumar, D., 2007. Thermally sprayable polyethylene coatings for marine environment. Prog Org Coat 60, 186–193.
[38] Chen, M.C., Koh, P.W., Ponnusamy, V.K., Lee, S.L., 2022. Titanium dioxide and other nanomaterials based antimicrobial additives in functional paints and coatings: Review. Prog Org Coat 163, 106660.
[39] Turner, A., Ostle, C., Wootton, M., 2022. Occurrence and chemical characteristics of microplastic paint flakes in the North Atlantic Ocean. Sci Total Environ 806, 150375.
[40] Lejars, M., Margaillan, A., Bressy, C., 2012. Fouling release coatings: a nontoxic alternative to biocidal antifouling coatings. Chem Rev 112, 4347–4390.
[41] Almeida, E., Diamantino, T.C., Sousa, O.D., 2007. Marine paints: the particular case of antifouling paints. Prog Org Coat 59, 2–20.
[42] Bejgarn, S., MacLeod, M., Bogdal, C., Breitholtz, M., 2015. Toxicity of leachate from weathering plastics: an exploratory screening study with Nitocra spinipes. Chemosphere 132, 114e119.
[43] Hanun, J.N., Hassan, F., Jiang, J.J., 2021. Occurrence, fate, and sorption behavior of contaminants of emerging concern to microplastics: Influence of the weathering/aging process. J Environ Chem Eng 9, 106290.
[44 Banfield, T.A., 1955. Anti-corrosion methods and materials. In: The Painting of Ships. British Paints Ltd.,, British.
[45] Information Research Ltd., A Profile of the European Paint Industry 7th ed.; 1986, pp. 13.
[46 Hamilton, A.D.C., 1957. Modern marine paints. Corros Technol 11, 5–8.
[47] Itou, S., 2010. Introduction to pigments. J Jpn Soc Colour Mater 83 (7), 308–316.
[48] Sato, A., 2013. Painting of marine coatings - basic points to pay attention to in painting of marine coatings. J JIME 48 (1), 94–99.
[49] Guerguer, M., Naaman, e S., Edfouf, Z., Raccurt, O., Bouaouine, H., 2021. Chemical degradation and color changes of paint protective coatings used in solar glass mirrors. Coatings 11, 476.
[50] Szeto, W., Leung, M.K.H., Leung, D.Y.C., 2021. Recent developments of titanium dioxide materials for aquatic antifouling application. J Mar Sci Technol 26, 301–321.
[51] Imhof, H.K., Laforsch, C., Wiesheu, A.C., 2016. Pigments and plastic in limnetic ecosystems: a qualitative and quantitative study on microparticles of different size classes. Water Res 98, 64–74.
[52] Waku H. Composition of antifouling paint. Would Intellectual Property Organization WO2021/033705 A1; 25 February 2021. (In Japanese).
[53] Hasan, C.K., Turner, A., Readman, J., Frickers, T., 2014. Environmental risks associated with booster biocides leaching from spent anti-fouling paint particles in coastal environments. Water Environ Res 86, 12.
[54] Harino, H., Yamato, S., 2021. Distribution of antifouling biocides in a coastal area of Tanabe Bay, Japan. J Mar Biol Assoc UK 101, 49–59.
[55] Adeyeye, O., Xiao, C.L., Zhang, Z.H., Liang, X.J., 2020. State, source and triggering mechanism of iron and manganese pollution in groundwater of Changchun, Northeastern China. Environ Monit Assess 192, 619.
[56] Bhandari, J., Khan, F., Abbassi, R., Garaniya, V., 2015. Modelling of pitting corrosion in marine and offshore steel structures – a technical review. J Loss Prev Process Ind 37, 39–62.
[57] Gronostajski, Z., Kaszuba, M., Widomski, P., Smolik, J., Ziemba, J., 2019. Analysis of wear mechanisms of hot forging tools protected with hybrid layers performed by nitriding and PVD coatings deposition. Wear 420–421, 269–280.
[58] Tian, Y.S., Chen, C.Z., Li, S.T., Huo, Q.H., 2005. Research progress on laser surface modification of titanium alloys. Appl Surf Sci 242, 177–184.
[59] Damborenea, J., 1998. Surface modification of metals by high power lasers. Surf Coat Tech 100–101, 377–382.
[60] Tian, J.Y., Xu, P., Chen, J.H., Liu, Q.B., 2019. Microstructure and phase transformation behaviour of a Fe/Mn/Si/Cr/Ni alloy coating by laser cladding. Opt Laser Eng 122, 97–104.
[61] Gao, S.L., Liang, J., Zhou, J.S., 2022. Evolution in microstructure features and properties of Mo-containing Fe-Cr-Ni-B-Si composite coatings by laser cladding. Mater Charact 188, 111926.
[62] Yang, J.X., Miao, X.H., Wang, X.B., Yang, F., 2014. Influence of Mn additions on the microstructure and magnetic properties of FeNiCr/60% WC composite coating produced by laser cladding. Int J Refract Met H 46, 58–64.
[63] Zayed, A., Garbatov, Y., Guedes Soares, C., 2018. Corrosion degradation of ship hull steel plates accounting for local environmental conditions. Ocean Eng 163, 299–316.
[64] Amir, N.S., Yusof, N.Z., Ismail, R., 2021. Green and sustainable antibiofouling coatings: a review. Earth Env Sci 685, 012023.
[65] Oikonomou, E.K., Iatridi, Z., Moschakou, M., Damigos, P., Bokias, B., Kallitsis, J.K., 2012. Development of Cu^{2+}- and/or phosphonium-based polymeric biocidal materials and their potential application in antifouling paints. Prog Org Coat 75, 190–199.
[66] Amo, B., Blustein, G., Perez, M., García, M., Deya, M., Stupak, M., et al., 2008. A multipurpose compound for protective coatings. Colloid Surf A 324, 58–64.
[67] Kitahara, K.I., Nakata, H., 2020. Plastic additives as tracers of microplastic sources in Japanese road dusts. Sci Total Environ 736, 139694.
[68] Liu, H., Ding, C.L., Zhang, G.C., Guo, Y.Y., Song, Y.Y., Thangaraj, S., et al., 2023. Dissolved and particulate heavy metal pollution status in seawater and sedimentary heavy metals of the Bohai Bay. Mar Environ Pollut 191, 106158.